

**Effects of plasma density irregularities on the pitch angle scattering of radiation belt electrons by signals from ground based VLF transmitters**

T Bell, U Inan, P Pidyyachiy, P Kulkarni, Michel Parrot

► **To cite this version:**

T Bell, U Inan, P Pidyyachiy, P Kulkarni, Michel Parrot. Effects of plasma density irregularities on the pitch angle scattering of radiation belt electrons by signals from ground based VLF transmitters. *Geophysical Research Letters*, American Geophysical Union, 2008, 35 (19), pp.L19103. 10.1029/2008GL034834 . insu-01408661

**HAL Id: insu-01408661**

**<https://hal-insu.archives-ouvertes.fr/insu-01408661>**

Submitted on 5 Dec 2016

**HAL** is a multi-disciplinary open access archive for the deposit and dissemination of scientific research documents, whether they are published or not. The documents may come from teaching and research institutions in France or abroad, or from public or private research centers.

L'archive ouverte pluridisciplinaire **HAL**, est destinée au dépôt et à la diffusion de documents scientifiques de niveau recherche, publiés ou non, émanant des établissements d'enseignement et de recherche français ou étrangers, des laboratoires publics ou privés.

# Effects of plasma density irregularities on the pitch angle scattering of radiation belt electrons by signals from ground based VLF transmitters

T. F. Bell,<sup>1</sup> U. S. Inan,<sup>1</sup> D. Pidduyachiy,<sup>1</sup> P. Kulkarni,<sup>1</sup> and M. Parrot<sup>2</sup>

Received 16 June 2008; revised 12 August 2008; accepted 25 August 2008; published 4 October 2008.

[1] Recent DEMETER spacecraft observations show that VLF signals from the NPM transmitter in Hawaii often strongly excite quasi-electrostatic whistler mode waves as the NPM signals propagate upward through plasma density irregularities. As a result of the NPM wave energy loss to the quasi-electrostatic waves, the transmitter signals will arrive at the radiation belts with less intensity than predicted by present models of VLF wave propagation and will produce less pitch angle scattering of energetic electrons than presently believed. This type of wave energy loss may be partially responsible for the pervasive wave intensity deficit for VLF transmitter signals in the plasmasphere recently noted by Starks et al. (2008). **Citation:** Bell, T. F., U. S. Inan, D. Pidduyachiy, P. Kulkarni, and M. Parrot (2008), Effects of plasma density irregularities on the pitch angle scattering of radiation belt electrons by signals from ground based VLF transmitters, *Geophys. Res. Lett.*, 35, L19103, doi:10.1029/2008GL034834.

## 1. Introduction

[2] On the basis of analytical models, it is commonly believed that VLF signals from powerful ground based transmitters determine the lifetimes of energetic radiation belt electrons (100 keV–1.5 MeV) on L shells in the range 1.3–2.8 [e.g., *Abel and Thorne, 1998; Millan and Thorne, 2007*]. The primary mechanism of interaction is pitch angle scattering during gyro-resonance, where the resonance condition can be expressed:

$$v_z = (m\omega_{ce}/\gamma - \omega)/k_z \quad (1)$$

where  $v_z$  is the component of the electron velocity along  $\mathbf{B}_0$ , the Earth's magnetic field,  $m$  is an integer,  $\omega_{ce}$  is the electron gyro-frequency,  $\omega$  is the wave frequency,  $\gamma = 1/\sqrt{1 - v^2/c^2}$ ,  $c$  = velocity of light, and  $k_z$  is the component of the wave vector  $\mathbf{k}$  along  $\mathbf{B}_0$ . As a result of the pitch angle scattering, energetic electrons are precipitated into the atmosphere at the base of the given  $L$  shell in both hemispheres.

[3] To test the hypothesis that VLF signals from ground based transmitters determine the lifetimes of energetic radiation belt electrons, one needs to know the characteristics of the VLF signals in the radiation belts, as well as the characteristics of the energetic electron precipitation pro-

duced by these VLF signals. To these ends, Stanford University has recently carried out a series of experiments in which the 21.4 kHz signals from the US Navy transmitter in Hawaii (NPM) are keyed in a regular OFF/ON pattern designed to reveal the characteristics of the radiated signals and the characteristics of any energetic electron precipitation that may be attributed to the transmitter signals.

[4] The subject of the present paper concerns the characteristics of the 21.4 kHz NPM signals as observed on the DEMETER spacecraft [*Parrot, 2006*] at  $\approx 700$  km altitude. In general, the wave intensity in the radiation belts can be determined from these input signals using well known raytracing techniques [e.g., *Bortnik et al., 2006*]. However raytracing methods will fail if the input signals couple to other wave modes along their propagation path, as we discuss below.

## 2. Observations

[5] The DEMETER plasma wave instrument (ICE) [*Berthelier et al., 2006*] was used to detect the 21.4 kHz VLF signals from NPM. The upper end of the nominal DEMETER plasma wave passband is 20 kHz. However, because of the high intensity of the NPM signals, they are aliased into the passband with observable intensity at a frequency of 18.4 kHz. The observed intensity of the 21.4 kHz signals is reduced  $\approx 10$  dB below their actual intensity because of the action of the anti-aliasing filter in the wave instrument.

[6] DEMETER plasma wave observations were carried out in the regions where NPM-induced energetic electron precipitation was expected. This precipitation is believed to occur through gyro-resonance and Landau resonance interactions, the conditions for which are given in (1). Since particle pitch angle scattering tends to be strongest near the magnetic equatorial plane where the gradients in  $\mathbf{B}_0$  are smallest, the precipitation regions were predicted to be roughly centered about the magnetic field line intercepted by the wave ray path from NPM as it crossed the magnetic equatorial plane. Ray tracing studies suggest that the intersection of the ray with the magnetic equator takes place at  $L \approx 1.9$ .

[7] DEMETER plasma wave observations were carried out over the presumed precipitation region north of NPM, as well as over the presumed precipitation region in the southern hemisphere. In Figure 1 we show an 18–19 kHz frequency-time spectrogram of DEMETER plasma wave electric field data acquired near the magnetic field line intersecting the NPM transmitter on 22 November, 2007. The presence of aliased NPM pulses is clearly in evidence at 18.6 kHz. Each pulse is 5 seconds in length, followed by

<sup>1</sup>STAR Laboratory, Stanford University, Stanford, California, USA.

<sup>2</sup>LPCE, CNRS, Orleans, France.

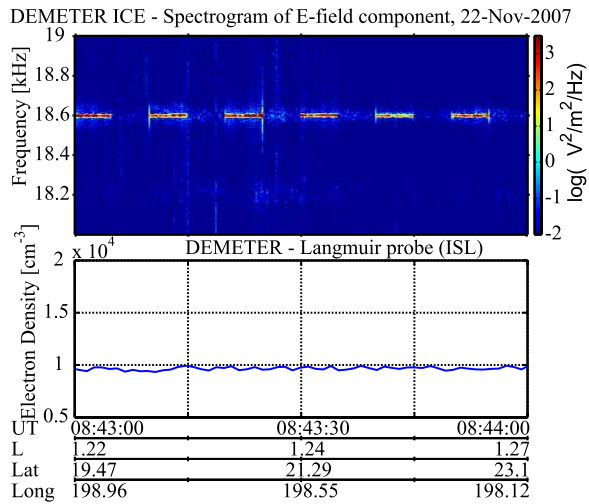


**Figure 1.** (top) Frequency-time spectrogram of the electric field of 5-second-duration pulses from the VLF transmitter NPM on 22 November 2007. (bottom) Local electron density as measured by the ISL instrument.

5 seconds in which no transmissions are made. This format also applies to Figures 2 and 3.

[8] Also present in Figure 1 is a plot of the background thermal electron density  $N_e$  as measured on the DEMETER ISL instrument [Lebreton *et al.*, 2006]. This density is measured once per second, and the distance between samples is roughly 8 km. It can be seen from the plot that the maximum fluctuation in  $N_e$  is  $\sim 10\%$ .

[9] Figure 2 shows an 18–19 kHz spectrogram of DEMETER plasma wave data acquired in the presumed northern precipitation region over a 60 second time period on 19 May, 2005. In Figure 2, the NPM pulses are partially obscured by signals transmitted by another VLF transmitter located in Australia. The center frequency of the signals from the Australian transmitter is 18.6 kHz, and the bandwidth of the signals is  $\sim 100$  Hz.

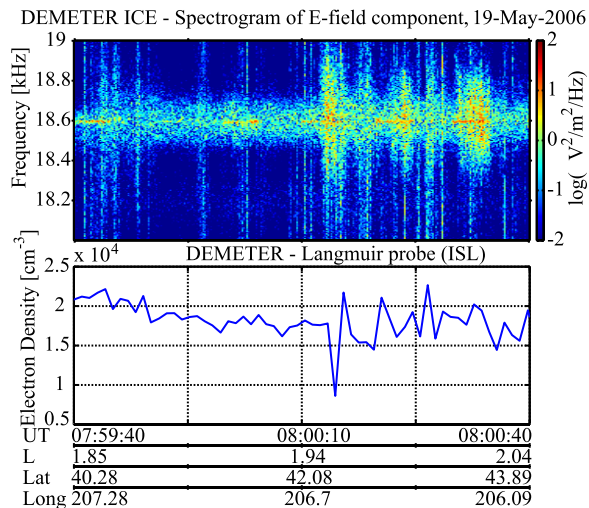


**Figure 2.** (top) Frequency-time spectrogram of the electric field of 5-second-duration pulses from the VLF transmitter NPM on 19 May 2006. (bottom) Local electron density as measured by the ISL instrument.

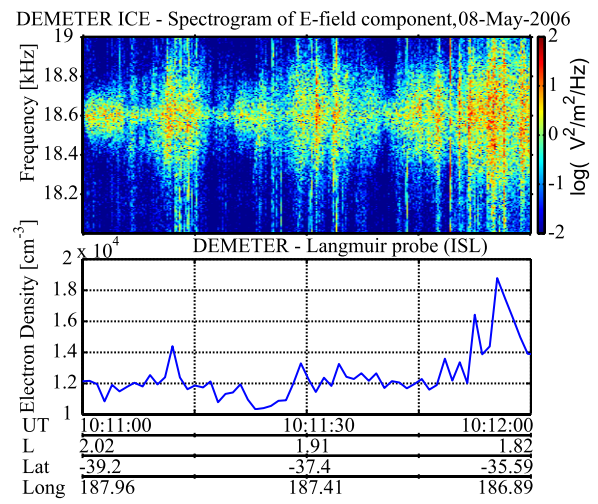


**Figure 3.** (top) Frequency-time spectrogram of the electric field of 5-second-duration pulses from the VLF transmitter NPM on 8 May 2006. The lower panel shows the local electron density as measured by the ISL instrument.

[10] The band width of the NPM pulses increases dramatically from a few Hz to  $\sim 1$  kHz at  $\sim 08:00:14$ , beginning at the same time as a large decrease occurs in  $N_e$ . Thereafter, the NPM apparent signal bandwidth varies irregularly as  $N_e$  exhibits large fluctuations.

[11] Figure 3 shows an 18–19 kHz spectrogram of DEMETER plasma wave data acquired in the presumed southern precipitation region on 08 May, 2006. The NPM signal bandwidth is as large as 1 kHz during the period, 10:11:00–10:12:00 UT, in which  $N_e$  exhibits large fluctuations. The largest bandwidth increase in the NPM signals occurs during the period in which the largest density fluctuations occur.

[12] Figure 4 is a map of the region surrounding NPM. The subsatellite tracks for the passes on which the wave data shown in Figures 1, 2, and 3 were obtained are shown

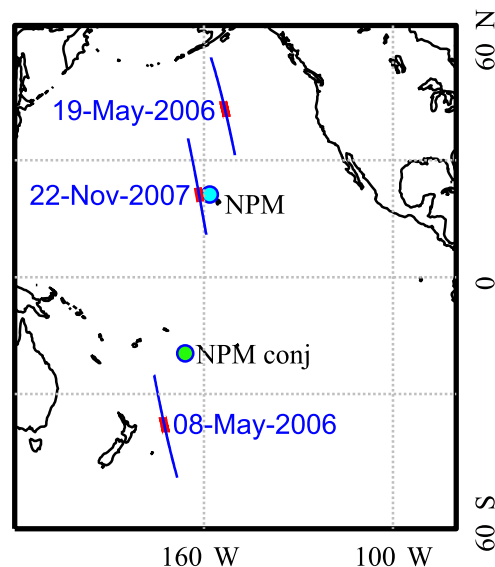


**Figure 4.** Map showing location of NPM and sub-satellite track of DEMETER during data acquisition.

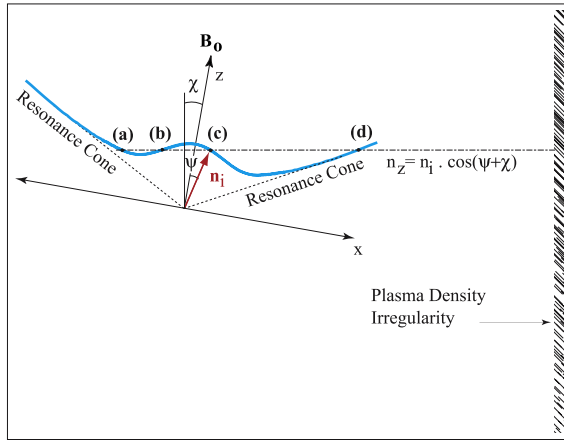


**Figure 5.** Plot showing the whistler mode refractive index surface and the refractive index of the incident, reflected, and transmitted waves during scattering from a planar plasma density irregularity.

by blue lines. The portions on which the displayed data was acquired are shown in red.

[13] During the period January–December 2006, observations of NPM signals were carried out on DEMETER 60 times in the southern precipitation region and 60 times in the northern precipitation region. For each pass, plasma wave data were acquired over a 6 minute interval, while the spacecraft traveled approximately 3000 km. Large NPM signal bandwidth increases in the presence of large plasma density fluctuations, such as those shown in Figures 2 and 3, were observed on approximately 35% of these passes.

### 3. Mechanism of Bandwidth Increase

[14] The large and irregular bandwidth increases in the NPM pulses shown in Figures 2 and 3 are very similar to those seen in the past in fixed frequency pulses from the Omega, North Dakota, ground based VLF transmitter [Bell *et al.*, 1994]. The Omega signals were observed by the COSMOS 1809 and DE-1 spacecraft at the respective altitudes of 1600 km and 950 km. The observed bandwidth increase was as large as 2 kHz. In this early work the bandwidth increases were attributed to the presence of quasi-electrostatic (QE) whistler mode waves excited by the transmitter pulses as they propagated through regions containing small scale (2–100 meters), magnetic-field-aligned, plasma density irregularities. The QE waves are excited through linear mode coupling as the input pulse scatters from the irregularities. As a result of the small wavelength of the QE waves, they are observed on moving spacecraft with a large Doppler shift.

[15] The excitation process can be understood from a simple application of Snell's law to the case of a whistler mode wave scattering from a plasma density irregularity, as detailed in Figure 5, which shows a cross section of the refractive index surface (blue) for an input electromagnetic (EM) whistler mode wave. The refractive index surface is generated by plotting the refractive index  $n(\psi)$  as a function of the wave normal angle  $\psi$ . It is assumed that the wave vector  $\mathbf{k}$  lies in the plane of the paper, and that the planar irregularity lies in a plane perpendicular to the plane of the

paper. Thus the normal to the planar irregularity also lies in the plane of the paper

[16] The component of the refractive index parallel to the surface of the irregularity is:  $n_z = n_i(\psi) \cos(\psi + \chi)$ , where  $n_i(\psi)$  is the refractive index of the input wave and  $\chi$  is the angle between  $\mathbf{B}_0$  and the plane of the irregularity. By Snell's law,  $n_z$  must be the same for the input wave plus all transmitted and reflected waves. If we draw the level line  $n_z = \text{constant}$ , we see from the  $n(\psi)$  surface that there are four possible solutions, (a), (b), (c), and (d). Solutions (c) and (b) represent the input EM wave and the reflected EM wave. Solutions (a) and (d) represent reflected and transmitted QE waves. Because of the tilt of the irregularity with respect to  $\mathbf{B}_0$ , one of the excited QE waves has a larger refractive index than the other. This larger value is necessary in order to achieve the largest Doppler shifts observed.

[17] According to Stix [1962], the resonance cone angle  $\psi_r$  is defined through the relation:  $\tan \psi_r = \sqrt{-P/S}$ , where the plasma parameters  $P$  and  $S$  are defined in Stix [1962]. In the case of the data shown in Figures 1, 2, and 3, we have  $P \simeq -f_o^2/f^2$ ,  $S \simeq f_o^2/f_{ce}^2$ , and  $\tan \psi \simeq f_{ce}/f$ , where  $f_o$  is the electron plasma frequency,  $f_{ce}$  is the electron gyrofrequency, and  $f$  is the wave frequency. Noting from Figure 5 that for the QE waves  $\psi \simeq \psi_r$ , we can find a simple expression for the value of the refractive index for the QE waves,  $n_{lh}$ , for the case in which the irregularity is aligned with  $\mathbf{B}_0$ :  $n_{lh} \simeq n_i \cos \psi_i / \cos \psi_r = n_i \cos \psi_i \sqrt{1 + f_{ce}^2/f^2}$ . In the case of grazing incidence with  $\psi_i \simeq 0$ , we can use the value of  $n_i$  appropriate for propagation along  $\mathbf{B}_0$ :  $n_i \simeq f_o \sqrt{f(f_{ce} - f)}$ . Assuming that  $N_e = 2 \cdot 10^4$ , as in Figure 2, then  $f_o \simeq 1.3$  MHz. In a centered dipole model,  $f_{ce} \simeq 850$  MHz at the DEMETER position shown in Figure 2. With these values we find  $n_i \simeq 10$ , and  $n_{lh} \simeq 400$ . The value of  $n_{lh}$  can be larger than 400 if the irregularity is not field aligned. From Figure 5 it can be shown that in general the largest value is:  $n_{lh} \simeq n_i \cos(\psi_i + \chi) / \cos(\psi_r + \chi)$ . The value of  $n_{lh}$  becomes arbitrarily large when  $\psi_r + \chi \simeq 90^\circ$ .

[18] The Doppler shift of a QE wave in the moving frame of DEMETER is:  $\delta f = \mathbf{k}_{lh} \cdot \mathbf{v}_{sc} / 2\pi$ , where  $\mathbf{v}_{sc}$  is the spacecraft velocity vector whose magnitude is  $\simeq 8$  km/s. For  $f \ll f_{ce}$ , the wave vectors of the two excited QE waves are approximately anti-parallel, and will be observed on DEMETER with equal and opposite doppler shifts when the irregularity is parallel to  $\mathbf{B}_0$ . The dip angle at DEMETER near  $L \simeq 2$  is approximately  $65^\circ$ , and thus the angle between  $\mathbf{k}_{lh}$  and  $\mathbf{v}_{sc}$  is small. In this case  $\delta f \simeq n_{lh} f v_{sc} / c \simeq 200$  Hz, and the total apparent signal bandwidth will be 400 Hz. If it is assumed that the plasma density irregularities are tilted  $1^\circ$  with respect to  $\mathbf{B}_0$  (i.e.,  $\chi = 1^\circ$ ), then the two refractive indices for the QE waves will be  $n_{lh1} \simeq 1400$  and  $n_{lh2} = 240$ . The total apparent bandwidth increase in this case would be  $\delta f \simeq 800$  Hz. Additional discussion of the effects of tilted planar irregularities can be found in work by Bell *et al.* [2004].

### 4. Discussion

[19] As the NPM signals scatter from the plasma density irregularities, wave energy is transferred from the NPM signals to the excited QE waves. This energy transfer thus represents a loss mechanism for the NPM signals. Consequently, when the NPM signals reach the magnetic equatorial plane they

will have a smaller amplitude than that predicted by models which do not take the irregularities into account [e.g., *Abel and Thorne*, 1998].

[20] This type of wave energy loss may be partially responsible for the wave intensity deficit recently noted by *Starks et al.* [2008], who found that VLF signals from ground-based communications transmitters, such as NPM, have an observed intensity on various spacecraft which, on average, is approximately 20 dB below that predicted by present models of VLF wave transionospheric propagation.

[21] Although the input NPM waves may lose energy to QE waves, this does not necessarily imply that the total energetic electron pitch angle scattering will be significantly less, since the excited QE waves can also cause pitch angle scattering if they reach the magnetic equatorial plane. The principal damping mechanism for the QE waves is Landau damping [*Bell et al.*, 2004].

[22] The distance over which the NPM signals can propagate before losing substantial power depends upon the irregularity structure. For the case of weak scattering in which the plasma density irregularities are small (e.g.,  $\delta N/N_o \simeq 2\%$ ), and well separated, it has been estimated [*Bell and Ngo*, 1990] that 15 kHz waves can propagate approximately 3000 km within the irregularity field before losing 4.5 dB of power. In the case of strong scattering where significant irregularities exist along the entire propagation path, it can be expected that the initial wave energy of the NPM signals will be distributed between a number of QE and EM wave modes.

[23] On the basis of the DEMETER plasma wave and thermal electron density observations, we conclude that VLF signals from ground based transmitters may be subject to significant energy loss through the excitation of QE whistler mode waves. This type of wave attenuation needs to be included in realistic models of the effects of VLF transmitter signals on radiation belt electrons.

[24] **Acknowledgments.** The Stanford University STAR Laboratory is a guest investigator of the French micro-satellite DEMETER operated by Centre National d'Etudes Spatiales (CNES). The Stanford authors were supported by the Department of the Air Force, under grant F49620-03-1-0338-P00002 and contract F19628-03-C-0059-P00002 and by the Office of Naval Research under Prime Award N000140710789 to the University of Maryland with subcontract Z882802 to Stanford.

## References

- Abel, B., and R. M. Thorne (1998), Electron scattering loss in Earth's inner magnetosphere: 1. Dominant physical processes, *J. Geophys. Res.*, *103*, 2385.
- Bell, T. F., and H. D. Ngo (1990), Electrostatic lower hybrid waves excited by electromagnetic whistler mode waves scattering from planar magnetic-field-aligned plasma density irregularities, *J. Geophys. Res.*, *95*, 149.
- Bell, T. F., U. S. Inan, D. Lauben, V. S. Sonwalkar, R. A. Helliwell, Y. P. Sobolev, V. M. Chmyrev, and S. Gonzalez (1994), DE-1 and COSMOS 1809 observations of lower hybrid waves excited by VLF whistler mode waves, *Geophys. Res. Lett.*, *21*, 653.
- Bell, T. F., U. S. Inan, M. Platino, J. S. Pickett, P. A. Kossey, and E. J. Kennedy (2004), CLUSTER observations of lower hybrid waves excited at high altitudes by electromagnetic whistler mode signals from the HAARP facility, *Geophys. Res. Lett.*, *31*, L06811, doi:10.1029/2003GL018855.
- Berthelier, J. J., et al. (2006), ICE, the electric field experiment on DEMETER, *Planet. Space Sci.*, *54*, 456.
- Bortnik, J., U. S. Inan, and T. F. Bell (2006), Temporal signatures of radiation belt electron precipitation induced by lightning-generated MR whistler waves: 1. Methodology, *J. Geophys. Res.*, *111*, A02204, doi:10.1029/2005JA011182.
- Lebreton, J.-P., et al. (2006), The ISL Langmuir probe experiment processing onboard DEMETER: Scientific objectives, description, and first results, *Planet. Space Sci.*, *54*, 472.
- Millan, R. M., and R. M. Thorne (2007), Review of radiation belt relativistic electron losses, *J. Atmos. Sol. Terr. Phys.*, *69*, 362.
- Parrot, M. (2006), Special issue of *Planetary and Space Science* 'DEMETER', *Planet. Space Sci.*, *54*, 411.
- Starks, M. J., R. A. Quinn, G. P. Ginot, J. M. Albert, G. S. Sales, B. W. Reinisch, and P. Song (2008), Illumination of the plasmasphere by terrestrial very low frequency transmitters: Model validation, *J. Geophys. Res.*, doi:10.1029/2008JA013112, in press.
- Stix, T. H. (1962), *The Theory of Plasma Waves*, McGraw-Hill, New York.
- T. F. Bell, P. Kulkarni, D. Piddiyachiy, and U. S. Inan, STAR Laboratory, Stanford University, Stanford, CA 94305, USA. (bell@nova.stanford.edu)
- M. Parrot, LPCE, CNRS, 3A Avenue de la Recherche Scientifique, F-45071 Orleans CEDEX 2, France.